



This article appeared in a journal published by Elsevier. The attached copy is furnished to the author for internal non-commercial research and education use, including for instruction at the authors institution and sharing with colleagues.

Other uses, including reproduction and distribution, or selling or licensing copies, or posting to personal, institutional or third party websites are prohibited.

In most cases authors are permitted to post their version of the article (e.g. in Word or Tex form) to their personal website or institutional repository. Authors requiring further information regarding Elsevier's archiving and manuscript policies are encouraged to visit:

<http://www.elsevier.com/copyright>



Contents lists available at ScienceDirect

Electrochimica Acta

journal homepage: www.elsevier.com/locate/electacta

Electrochemical performance of high specific capacity of lithium-ion cell $\text{LiV}_3\text{O}_8//\text{LiMn}_2\text{O}_4$ with LiNO_3 aqueous solution electrolyte

Mingshu Zhao^{a,*}, Qingyang Zheng^b, Fei Wang^a, Weimin Dai^a, Xiaoping Song^a^a MOE Key Laboratory for Nonequilibrium Synthesis and Modulation of Condensed Matter, School of Science, Xi'an Jiaotong University, 710049 Xi'an, China^b Xi'an High-tech Research Institute, 710025 Xi'an, China

ARTICLE INFO

Article history:

Received 16 December 2010

Received in revised form 5 February 2011

Accepted 12 February 2011

Available online 21 February 2011

Keywords:

Aqueous rechargeable lithium battery

Lithium manganese oxide

Lithium vanadium oxide

Specific capacity

Cycle ability

ABSTRACT

The electrochemical performance of aqueous rechargeable lithium battery (ARLB) with LiV_3O_8 and LiMn_2O_4 in saturated LiNO_3 electrolyte is studied. The results indicate that these two electrode materials are stable in the aqueous solution and no hydrogen or oxygen produced, moreover, intercalation/de-intercalation of lithium ions occurred within the range of electrochemical stability of water. The electrochemical performance tests show that the specific capacity of LiMn_2O_4 using as the cathode of ARLB is similar to that of ordinary lithium-ion battery with organic electrolyte, which works much better than the formerly reported. In addition, the cell systems exhibit good cycling performance. Therefore, it has great potential comparing with other batteries such as lead acid batteries and alkaline manganese batteries.

© 2011 Elsevier Ltd. All rights reserved.

1. Introduction

In the mid of 1990s, Dahn firstly put forward ARLB assumption, which has offered a brand-new research of the lithium ion battery [1–6]. Due to the safety problems of the organic electrolyte, it has much more restriction in the application of the traditional lithium ion battery. ARLB can solve the safety problems in some extents, which can assemble the battery without gas protection and humidity control. And the inorganic electrolyte is cheaper; the ion conductivity is two orders of magnitude higher than the organic electrolyte. Especially, the ARLB is the green environmental protection battery indeed [7–12].

There exist two problems in the ARLB system, such as lower specific capacity and bad cycle ability, and the reasons are not clear yet [13–16]. Therefore, in this paper, the preparation of the electrode materials and the electrochemical performances of the ARLB system are studied.

2. Experimental

2.1. Preparation

LiMn_2O_4 and LiV_3O_8 were synthesized using solid-step-sintering method as follows. Li_2CO_3 and MnO_2 were mixed with

molar of 0.51:2, and ground, pressed; then heated at 350 °C for 12 h and 800 °C for 24 h to prepare LiMn_2O_4 , labeled as A. The other LiMn_2O_4 sample was prepared by the above similar method, but the difference was used with $\text{C}_{12}\text{H}_{22}\text{O}_{11}$ (sucrose), which added with 20 wt% of the total mass of Li_2CO_3 and MnO_2 , marked as B. LiV_3O_8 was synthesized with Li_2CO_3 and V_2O_5 , mixed with molar of 1.02:6, and pressed, then sintered at 680 °C for 12 h and 350 °C for 8 h.

The synthesized materials were, respectively, mixed with acetylene black and polyvinylidene fluoride (PVDF) with the mass of 80:10:10, which were dissolved in 1-methyl-2-pyrrolidone (NMP). Then the black viscous slurry was ball-milled and dried at 80 °C for 2 h; then deposited onto Ni mesh and pressed into the thickness of 0.12 mm, and dried under vacuum at 100 °C for 10 h to obtain the electrode. The inorganic electrolyte was neutral saturated LiNO_3 aqueous solution. The ARLB system was fabricated in a 250 ml beaker, which were assembled with three electrodes. One was the working electrode using active materials electrode, the other was the counter electrode which made use of anode electrode, and another was reference electrode using with saturated calomel electrode (SCE).

2.2. Characterization techniques

The crystal phase structures of the samples were characterized using the Bruker D8-Advanced XRD with Cu K α radiation. The particle morphology was studied with a JEOL JSM-7000F instrument. The

* Corresponding author. Tel.: +86 29 8266 3034; fax: +86 29 8266 7872.

E-mail address: zhaomshu@mail.xjtu.edu.cn (M. Zhao).

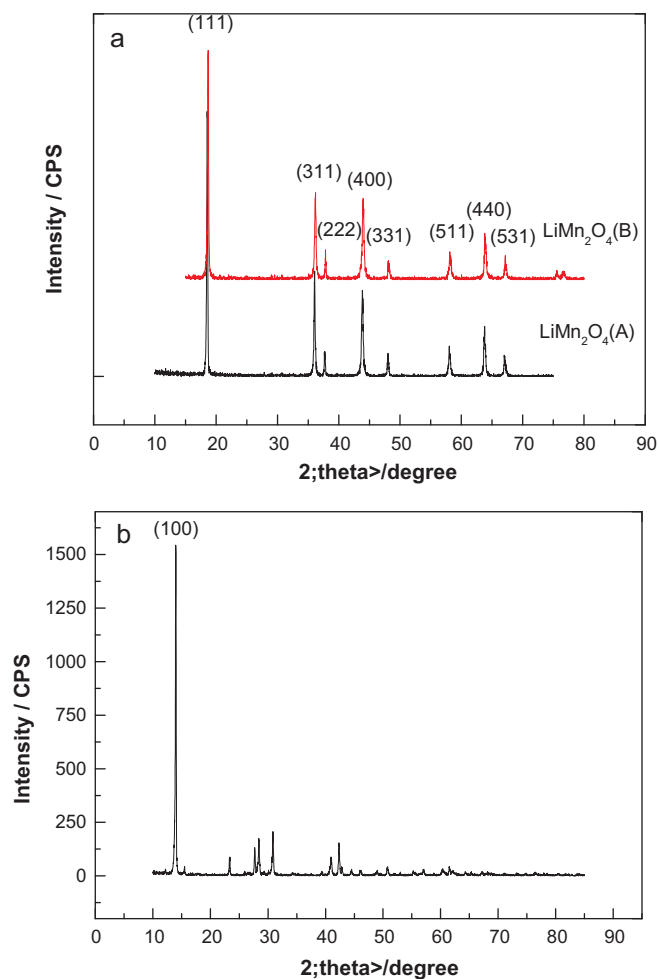


Fig. 1. The X-ray diffraction pattern of the materials. (a) LiMn_2O_4 and (b) LiV_3O_8 .

electrochemical properties were made using Arbin BT2000 instrument, and the testament software was Arbin MITS PRO.

3. Results and discussion

Fig. 1(a) shows the XRD patterns of LiMn_2O_4 samples having the spinel structure without any impurity phases, which belong to $\text{Fd}3\text{m}$ face cubic crystal system (ICSD, no. 087775). In this crystal structure, lithium atom occupies the tetragonal 8a position, manganese atom occupies 16d position, and oxygen atom is in the position of 32e. In Fig. 1(b), there is a characteristic peak of (100) existing at 13° for LiV_3O_8 , which shows that it has a layer structure.

Fig. 2 illustrates the SEM photos of the materials. The appearance of LiMn_2O_4 (B) grains is regular. Seen from Fig. 2(b), the grain size of the particles is less than $0.2\text{ }\mu\text{m}$. However, in Fig. 2(a), the particles of LiMn_2O_4 (A) have agglomeration. In Fig. 2(c), LiV_3O_8 has an obvious layer structure overlapping into column like, and there are many smaller granular grains on the surface of large particles.

Fig. 3 shows the cyclic voltammeter curves of the samples in saturated LiNO_3 aqueous electrolyte at a scan rate of 2 mV s^{-1} . In Fig. 3, the hydrogen evolution reaction locates at $E_{\text{SCE}} = -1.0\text{ V}$ and the oxygen evolution occurs at $E_{\text{SCE}} = 1.7\text{ V}$. For LiV_3O_8 , one couple of symmetrical redox peaks locates at $E_{\text{SCE}} = -0.5\text{ V}$ (red.1) and $E_{\text{SCE}} = 0.2\text{ V}$ (ox.1) which correspond to the intercalation and de-intercalation of lithium ions, then the average redox potential is -0.15 V (vs. SCE). As the hydrogen evolution reaction occurs at the more negative potential, LiV_3O_8 is more stable without hydrogen evolution in this solution, which can be used as the anode for

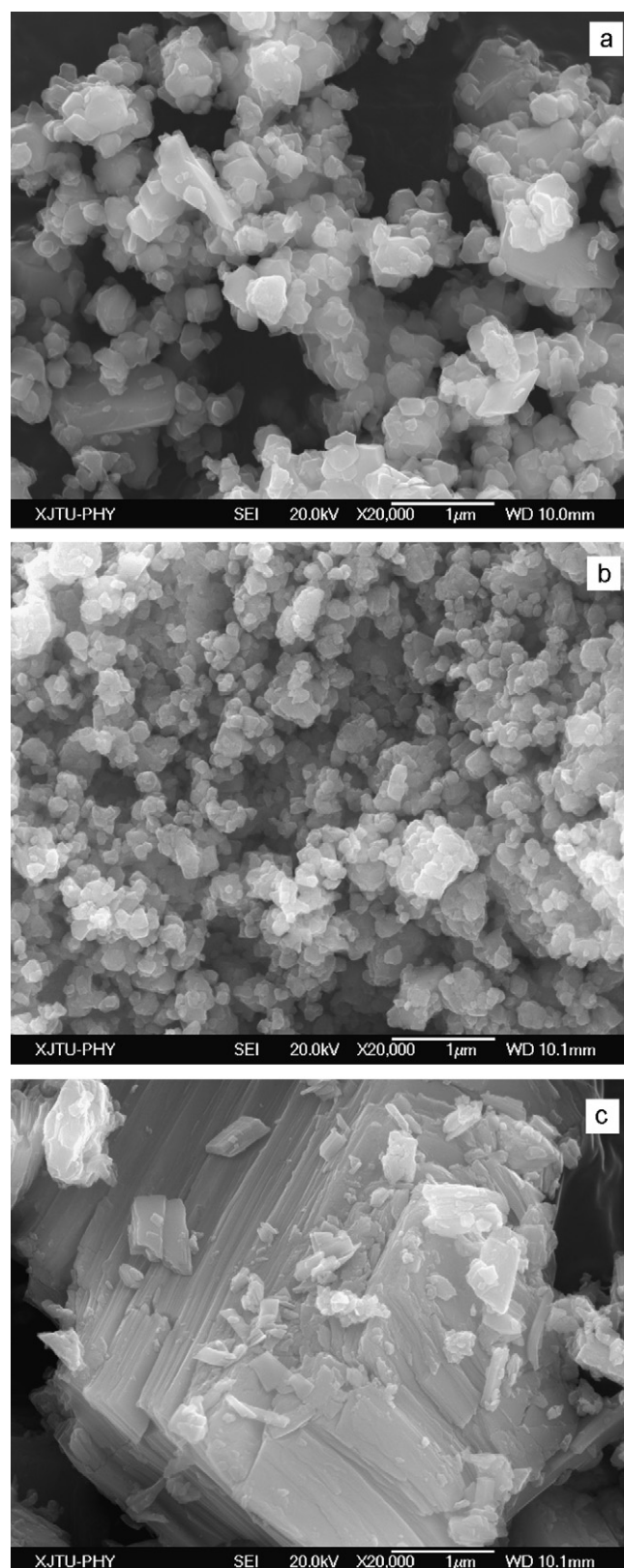


Fig. 2. The SEM photos of the materials. (a) LiMn_2O_4 (A), (b) LiMn_2O_4 (B), and (c) LiV_3O_8 .

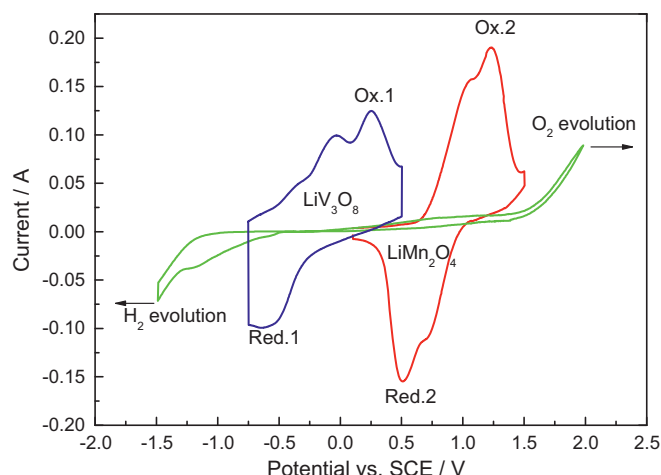


Fig. 3. The cyclic voltammeter curves of materials in saturated LiNO_3 aqueous electrolyte at a scan rate of 2 mV s^{-1} .

the ARLB. Meanwhile, there is a pair of corresponding redox peaks locates at $E_{\text{SCE}} = 0.5 \text{ V}$ and $E_{\text{SCE}} = 1.25 \text{ V}$ which ascribes to the de-intercalation and intercalation of lithium ion to LiMn_2O_4 . These potentials are lower than those of the oxygen evolution reaction, so LiMn_2O_4 can be acted as the cathode for the ARLB.

The 1st charge–discharge curves of $\text{LiV}_3\text{O}_8/\text{LiMn}_2\text{O}_4$ ARLBs are illustrated in Fig. 4. In Fig. 4, the potential difference is related to SCE, and these ARLB systems have two voltage plateaus. And the average charge and discharge voltages of $\text{LiV}_3\text{O}_8/\text{LiMn}_2\text{O}_4$ (A) ARLB are 0.92 V and 0.88 V , respectively. Meanwhile, those of $\text{LiV}_3\text{O}_8/\text{LiMn}_2\text{O}_4$ (B) ARLB are 0.95 V and 0.92 V separately. These data are accordance with the CV results.

The 1st charge and discharge specific capacities of LiMn_2O_4 (A) are 134.3 mAh g^{-1} and 113.5 mAh g^{-1} . As well, those of LiMn_2O_4 (B) are $127.46 \text{ mAh g}^{-1}$ and $120.28 \text{ mAh g}^{-1}$. Moreover, the coulombic efficiency of LiMn_2O_4 (B) is much larger than that of LiMn_2O_4 (A). Compared with other literature, the above results are good, for example, in Ref. [17], the 1st discharge specific capacities of $\text{LiV}_3\text{O}_8/\text{LiMn}_2\text{O}_4$ ARLB is 55.1 mAh g^{-1} , and in Ref. [18], that of $\text{LiV}_3\text{O}_8/\text{LiCoO}_2$ is 60 mAh g^{-1} , and higher than data in Refs. [4,19]. It is assumed that the higher 1st specific capacity in this paper is due to the much higher conductivity of the aqueous solution, the much smaller size of the particle, the larger specific surface, and the shorter distance of lithium ion's intercalation and de-intercalation.

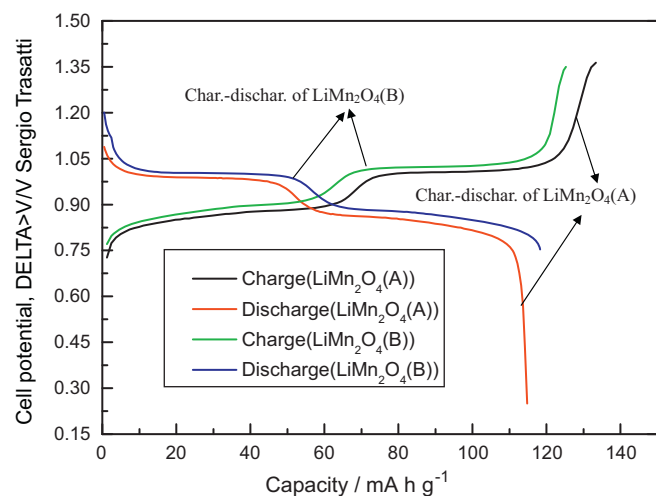


Fig. 4. The 1st charge–discharge curves of $\text{LiV}_3\text{O}_8/\text{LiMn}_2\text{O}_4$ (A) ARLB and $\text{LiV}_3\text{O}_8/\text{LiMn}_2\text{O}_4$ (B) ARLB.

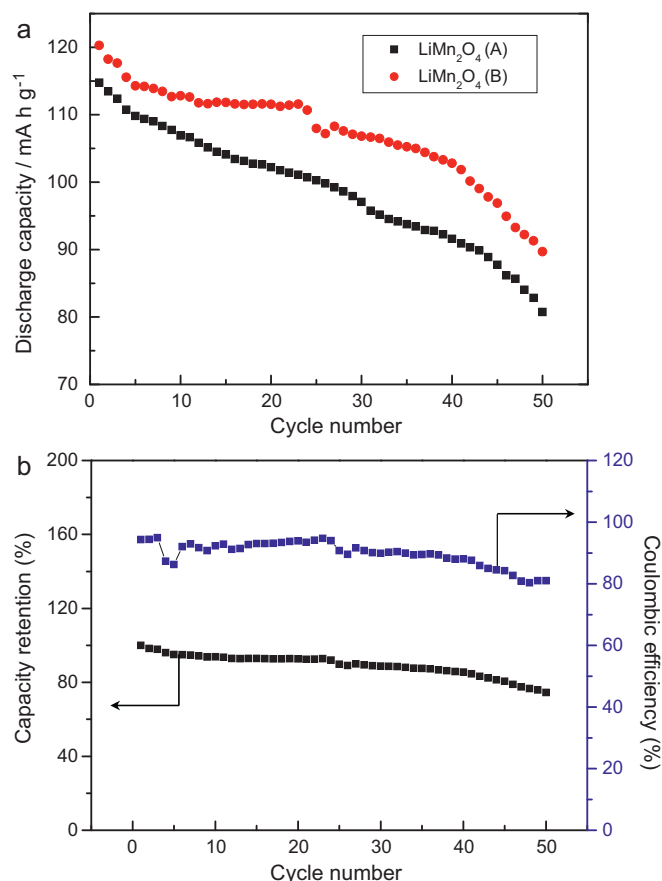


Fig. 5. The curves of discharge cyclic performance of $\text{LiV}_3\text{O}_8/\text{LiMn}_2\text{O}_4$ ARLB systems. (a) $\text{LiV}_3\text{O}_8/\text{LiMn}_2\text{O}_4$ ARLB systems and (b) the capacity retention and the coulombic efficiency of $\text{LiV}_3\text{O}_8/\text{LiMn}_2\text{O}_4$ (B) ARLB.

The discharge cyclic performance at 0.2C rate between 0.25 V and 1.4 V of the ARLB systems is shown in Fig. 5. For $\text{LiV}_3\text{O}_8/\text{LiMn}_2\text{O}_4$ (A) ARLB, the discharge specific capacity after 25 cycles is $100.29 \text{ mAh g}^{-1}$, and the capacity retention is 88.1% . While after 42 cycles, the discharge specific capacity is 90.33 mAh g^{-1} , and the capacity retention is 78.7% . For $\text{LiV}_3\text{O}_8/\text{LiMn}_2\text{O}_4$ (B) ARLB, the discharge specific capacity after 24 cycles is $110.66 \text{ mAh g}^{-1}$, and the capacity retention is 92% , and more importantly, the coulombic efficiency is 94% . While after 42 cycles, the discharge specific capacity is still $100.16 \text{ mAh g}^{-1}$, and the capacity retention is 83.27% , specially, the coulombic efficiency is 85.96% . In Fig. 5(b), the coulombic efficiency in the latter cycles is below 100% , the main side reaction maybe an interaction between the lithium ions and electrode surface, especially between the aqueous electrolyte and electrode surface. Electrode surface state will basically play an important role on the kinetics of charge transfer reaction, and it means that the interaction between the surface of LiMn_2O_4 active materials and LiNO_3 aqueous electrolyte determine the activation energy in the process of the electrode reaction [20]. But, the irreversible capacity loss in organic electrolyte solutions is attributed to the formation of protective solid electrolyte film (SEI) on the surface of electrode material, due to the decomposition of the electrolyte in the surface of electrode active materials [21–24]. We cannot identify what kind of interaction is presented between them and perhaps the interaction between the lithium ion and organic solvent is so strong that this interaction may not affect the activation energy in many cases, then may not increase the charge transfer resistance [20].

Moreover, it can also be seen from Fig. 5 that the recycle performance of the $\text{LiV}_3\text{O}_8/\text{LiMn}_2\text{O}_4$ (B) ARLB is better than that of the

$\text{LiV}_3\text{O}_8//\text{LiMn}_2\text{O}_4$ (A) ARLB. It can be inferred that $\text{C}_{12}\text{H}_{22}\text{O}_{11}$, which was used as the additive to prepare LiMn_2O_4 (B), has influenced the electrochemical performance of LiMn_2O_4 used for ARLB. During the sintering preparation process, it is presumed that, $\text{C}_{12}\text{H}_{22}\text{O}_{11}$ (sucrose) decomposes to carbon along with gas, and avoid particles to aggregate; moreover, resulting in carbon adhering to the surface of LiMn_2O_4 particle, and increasing its surface conductivity. Meanwhile, the gas generation leads LiMn_2O_4 particle loose, thus this LiMn_2O_4 (B) active materials electrode in the LiNO_3 solution decreases the charge transfer resistance without the presence of any other transition metal such as copper adsorption [20], then improves the electrochemical properties of this ARLB system using LiMn_2O_4 (B) as the cathode materials. And these reasons of $\text{C}_{12}\text{H}_{22}\text{O}_{11}$'s effects are needed to be studied systematically in our research.

In this paper, the cyclic performance of these ARLB systems is better than that of other ARLB systems in some literatures, for example, in Ref. [2], $\text{VO}_2//\text{LiMn}_2\text{O}_4$ only has 25 cycles, and in Ref. [4], the discharge capacity of ARLB decays 15% after 10 cycles, while decays 60% after 25 cycles. But to my knowledge, Prof. Xia of Fudan Univ., China reported better data in aqueous lithium ions battery [25].

4. Conclusions

In this paper, the recycle CV results show that whether LiMn_2O_4 or LiV_3O_8 can exist stably in the saturated LiNO_3 aqueous solution. Importantly, the 1st specific capacity and the cycle performance of the $\text{LiV}_3\text{O}_8//\text{LiMn}_2\text{O}_4$ ARLB are better than those of reported data in some references. Moreover, the effects of $\text{C}_{12}\text{H}_{22}\text{O}_{11}$ on the electrochemistry performance of LiMn_2O_4 used for ARLB are needed to be studied systematically.

Acknowledgements

The authors would like to acknowledge Xi'an Applied Materials Innovation Fund Application (XA-AM-2008-16), Xi'an Jiaotong Uni-

versity Inter-disciplinary Project Fund (0109-08140020) and the Province Natural Science Foundation of Shaan Xi (2010JM6018), and Xi'an Jiaotong University Graduate Student Innovates Fund for providing financial support to this work.

References

- [1] W. Li, J.R. Dahn, D. Wainwright, *Science* 264 (1994) 1115.
- [2] G. James, *Science* 264 (1994) 1084.
- [3] M. Broussely, J.P. Planchat, G. Rigobert, D. Virey, G. Sarre, J. Power Sources 68 (1997) 8.
- [4] W. Li, J.R. Dahn, *J. Electrochem. Soc.* 142 (1995) 1742.
- [5] G.X. Wang, S. Zhong, D.H. Bradhurst, S.X. Dou, H.K. Liu, *J. Power Sources* 74 (1998) 198.
- [6] Y. Xia, H. Takeshige, H. Noguchi, *J. Power Sources* 56 (1995) 61.
- [7] H.B. Wang, K.L. Huang, Y.Q. Zeng, S. Yang, L.Q. Chen, *Electrochim. Acta* 52 (2007) 3280.
- [8] J. Kohler, H. Makiyara, H. Uegaito, H. Inoue, M. Toki, *Electrochim. Acta* 46 (2000) 59.
- [9] A. Eftekhari, *Electrochim. Acta* 47 (2001) 495.
- [10] J.W. Lee, S.I. Pyun, *Electrochim. Acta* 49 (2004) 753.
- [11] M.M. Rao, M. Jayalakshmi, O. Schaf, H. Wuff, U. Guth, F. Scholz, *J. Solid State Electrochem.* 5 (2001) 50.
- [12] K.S. Abou-El-Sherbini, M.H. Askar, *J. Solid State Electrochem.* 7 (2003) 435.
- [13] M. Jayalakshmi, M.M. Rao, F. Scholz, *Langmuir* 19 (2003) 8403.
- [14] Y.P. Wu, X.B. Dai, J.Q. Ma, Y.J. Cheng, *Lithium Ion Batteries: Practice and Applications*, 1st ed., Chemical Industry Press, Beijing, 2004.
- [15] K.M. Shaju, P.G. Bruce, *Adv. Mater.* 18 (2006) 2330.
- [16] G.J. Wang, L.J. Fu, N.H. Zhao, L.C. Yang, Y.P. Wu, H.Q. Wu, *Angew. Chem. Int. Ed.* 46 (2007) 295.
- [17] G.J. Wang, H.P. Zhang, L.J. Fu, B. Wang, Y.P. Wu, *Electrochem. Commun.* 9 (2007) 1873.
- [18] G.J. Wang, N.H. Zhao, L.C. Yang, Y.P. Wu, H.Q. Wu, *Electrochim. Acta* 52 (2007) 4911.
- [19] X.H. Liu, T. Saito, T. Doi, S. Okada, J. Yamaki, *J. Power Sources* 189 (2009) 706.
- [20] N. Nakayama, I. Yamada, Y. Huang, T. Nozawa, Y. Iriyamac, T. Abea, Z. Ogumia, *Electrochim. Acta* 54 (2009) 3428.
- [21] I.B. Stojkovic, N.D. Cvjeticanin, S.V. Mentus, *Electrochem. Commun.* 12 (2010) 371.
- [22] D. Aurbach, K. Gamolsky, B. Markovsky, Y. Gofer, M. Schmidt, U. Heider, *Electrochim. Acta* 47 (2002) 1423.
- [23] H. Ota, K. Shima, M. Ue, J. Yamaki, *Electrochim. Acta* 49 (2004) 565.
- [24] E.G. Shim, T.H. Nam, J.G. Kim, H.S. Kim, S.I. Moon, *J. Power Sources* 172 (2007) 901.
- [25] J.Y. Luo, W.J. Cui, P. He, Y.Y. Xia, *Nat. Chem.* 2 (2010) 760.